

Stability of Dynamically Collapsing Gas Sphere

Tomoyuki HANAWA

*Department of Astrophysics, Nagoya University, Chikusa-ku, Nagoya 464-8602**E-mail(TH): hanawa@a.phys.nagoya-u.ac.jp and*

Tomoaki MATSUMOTO

*Faculty of Liberal Arts, Hosei University, Fujimi, Chiyoda-ku, Tokyo 102-8160**E-mail(TH): matsu@i.hosei.ac.jp*

(Received ; accepted)

Abstract

We discuss stability of dynamically collapsing gas spheres. We use a similarity solution for a dynamically collapsing sphere as the unperturbed state. In the similarity solution the gas pressure is approximated by a polytrope of $P = K\rho^\gamma$. We examine three types of perturbations: bar ($\ell = 2$) mode, spin-up mode, and Ori-Piran mode. When $\gamma < 1.097$, it is unstable against bar-mode. It is unstable against spin-up mode for any γ . When $\gamma < 0.961$, the similarity solution is unstable against Ori-Piran mode. The unstable mode grows in proportion to $|t - t_0|^{-\sigma}$ while the central density increases in proportion to $\rho_c \propto (t - t_0)^{-2}$ in the similarity solution. The growth rate, σ is obtained numerically as a function of γ for bar mode and Ori-Piran mode. The growth rate of the bar mode is larger for a smaller γ . The spin-up mode has the growth rate of $\sigma = 1/3$ for any γ .

Key words: Gravitation — Hydrodynamics — ISM: clouds — Stars: formation

1. Introduction

As well as the majority of nearby pre-main sequence stars, most young stars have their companions (see, e.g., Mathieu 1994). Since even young protostars have their companions, fragmentation is more plausible for formation of multiple star systems than capture and other processes.

Fragmentation during the star formation has been paid much attention and a number of numerical simulations have been performed for clarifying it. Nonetheless the results are not conclusive. Some early simulations have only limited spatial resolution and their results on fragmentation are unreliable (Truelove et al. 1997). A gas cloud fragments artificially in numerical simulations of low resolution. If we exclude the artificial fragmentation, fragmentation proceeds but only slowly in numerical simulations. Fragmentation competes with the total collapse of a cloud. A cloud collapses and the density increases before it fragments. Only when an initial model was very much elongated, the simulation showed fragmentation of a cloud at a relatively low density. This initial model is, however, not applicable to a roundish dense core containing a binary.

Fragmentation has been studied not only by numerical simulations but also by linear stability analyses. While numerical simulations are advantageous at handling non-linearity, linear stability analyses are helpful for elucidating underlying physics. In this sense these two technolo-

gies are complementary. Most linear stability analyses thus far, however, deal with the stability of an equilibrium cloud against small perturbation. The competition with the total collapse could not be taken account into them. Silk, Suto (1988) tried to compute the stability of a similarity solution for the collapse of an isothermal gas cloud but could not obtain a self-consistent solution. Only recently Hanawa, Matsumoto (1999) succeeded in analyzing the stability of a collapsing isothermal cloud against non-spherical perturbations. They found that a collapsing isothermal cloud is unstable against bar mode ($\ell = 2$) perturbation. The bar mode grows in proportion to $\rho_c^{0.354}$ where ρ_c denotes the central density. When it grows, a collapsing gas cloud may change its shape from sphere to filament. This result is consistent with recent three-dimensional simulations by Truelove et al. (1998) and Matsumoto, Hanawa (1999) in which a filament forms in a collapsing cloud. The former showed that the filament fragments to form a binary. Thus the bar mode is interesting for understanding fragmentation during the collapse.

In this paper we extend the linear stability analyses of Hanawa, Matsumoto (1999) for collapsing non-isothermal spheres. For simplicity we employ the polytropic relation, $P = K\rho^\gamma$, for the model cloud. The polytrope model can describe temperature change during the collapse in the most simple form. The polytrope model of $\gamma \simeq 4/3$ can be applied also to a collapsing

iron core resulting Type II supernova. In section 2 we present the similarity solution for gravitationally collapsing sphere of a polytropic gas cloud. This section is essentially the review of Yahil (1983) and Suto, Silk (1991). We summarize their results to investigate the stability. In section 3 we examine the stability of the similarity solution against bar mode. The growth rate of the perturbation is larger when γ is smaller. The bar mode is degenerate and its growth rate is independent of the azimuthal wavenumber, m . The shape of the core suffering the bar mode depends on m and the sign of the perturbation. We show it visually. In section 4 we show that a spherically collapsing gas cloud is unstable against spin-up. This result is an extension of the stability analysis of Hanawa, Nakayama (1997). In section 6 we show that the similarity solution is unstable against a spherical perturbation when $\gamma < 0.961$. The analysis shown in section 5 is based on Ori, Piran (1988). A short summary is given in section 6.

2. Similarity Solution

For simplicity we consider gas of which equation of state is expressed by polytrope,

$$P = K \rho^\gamma, \quad (1)$$

where P and ρ denote the pressure and density, respectively. The hydrodynamical equations are then expressed as

$$\frac{\partial \rho}{\partial t} + \nabla \cdot (\rho \mathbf{v}) = 0 \quad (2)$$

and

$$\frac{\partial}{\partial t}(\rho \mathbf{v}) + \nabla P + \nabla \cdot (\rho \mathbf{v} \otimes \mathbf{v}) + \rho \nabla \Phi = 0, \quad (3)$$

where \mathbf{v} and Φ denote the velocity and gravitational potential, respectively. The gravitational potential is related with the density distribution by the Poisson equation,

$$\Delta \Phi = 4\pi G \rho, \quad (4)$$

where G denotes the gravitational constant.

For later convenience, we introduce the zooming coordinates of Bouquet et al. (1985) to solve equations (1) through (4). The zooming coordinates, $(\boldsymbol{\xi}, \tau)$, are related with the ordinary coordinates, (\mathbf{r}, t) , by

$$\begin{pmatrix} \boldsymbol{\xi} \\ \tau \end{pmatrix} = \begin{pmatrix} \frac{\mathbf{r}}{c_0 |t - t_0|} \\ -\ln |1 - t/t_0| \end{pmatrix}, \quad (5)$$

where c_0 denotes a standard sound speed and is a function of time t . The symbol, t_0 , denotes an epoch at the instant of the protostar formation. The density in the

zooming coordinates, ϱ , is related with that in the ordinary coordinates, ρ , by

$$\varrho(\mathbf{x}, \tau) = 4\pi G \rho (t - t_0)^2. \quad (6)$$

We define the standard sound speed, c_0 , so that it denotes the sound speed at a given t when $\varrho = 1$. Thus it is expressed as

$$c_0 = \sqrt{\gamma K} (4\pi G)^{(1-\gamma)/2} |t - t_0|^{1-\gamma}. \quad (7)$$

The pressure in the zooming coordinates, p , is related with the that in the ordinary coordinates, P , by

$$p = \frac{4\pi G}{c_0^2} P (t - t_0)^2. \quad (8)$$

Substituting equations (6) and (8) into equation (1), we obtain the polytrope relation in the zooming coordinates,

$$p = \frac{\varrho^\gamma}{\gamma}. \quad (9)$$

The velocity in the zooming coordinates, \mathbf{u} , is defined as

$$\mathbf{u} = \frac{\mathbf{v}}{c_0} + (2 - \gamma) \frac{\mathbf{r}}{c_0 |t - t_0|}. \quad (10)$$

This velocity denotes that with respect to the zooming coordinates, and includes the apparent motion, the last term in equation (10). The gravitational potential in the zooming coordinates, ϕ , is related with that in the ordinary coordinates, Φ by

$$\phi = \frac{\Phi}{c_0^2}. \quad (11)$$

In the zooming coordinates, the hydrodynamical equations are expressed as

$$\frac{\partial \varrho}{\partial \tau} + \nabla' \cdot (\varrho \mathbf{u}) = (4 - 3\gamma) \varrho, \quad (12)$$

$$\begin{aligned} \frac{\partial}{\partial \tau} (\varrho \mathbf{u}) + \nabla' \cdot (\varrho \mathbf{u} \otimes \mathbf{u}) + \nabla' p + \varrho \nabla' \phi \\ = (2 - \gamma)(\gamma - 1) \varrho \boldsymbol{\xi} + (7 - 5\gamma) \varrho \mathbf{1} \end{aligned} \quad (13)$$

and

$$\Delta' \phi = \varrho \quad (14)$$

for $t < t_0$. The symbols, ∇' and Δ' , denote the gradient and Laplacian in the $\boldsymbol{\xi}$ -space, respectively.

Assuming stationary in the zooming coordinates ($\partial/\partial\tau = 0$) and the spherical symmetry ($\partial/\partial\theta = \partial/\partial\varphi = 0$), we seek a similarity solution. Under these assumptions equations (12), (13), and (14) reduce to

$$\frac{\partial u_r}{\partial \xi} + \frac{u_r}{\varrho} \frac{\partial \varrho}{\partial \xi} = (4 - 3\gamma) - \frac{2u_r}{\xi}, \quad (15)$$

$$u_r \frac{\partial u_r}{\partial \xi} + \frac{1}{\varrho} \left(\frac{dp}{d\varrho} \right) \frac{\partial \varrho}{\partial \xi} + \frac{\partial \phi}{\partial \xi} = (2 - \gamma)(\gamma - 1) \xi + (3 - 2\gamma) u_r, \quad (16)$$

and

$$\frac{\partial \phi}{\partial \xi} = \frac{1}{\xi^2} \int_0^\xi \varrho(\zeta) \zeta^2 d\zeta = \frac{\varrho u_r}{4 - 3\gamma}, \quad (17)$$

where $\xi = |\mathbf{\xi}|$. After some algebra we can rewrite equations (15) and (16) into

$$\begin{aligned} (\varrho^{\gamma-1} - u_r^2) \left(\frac{d\varrho}{d\xi} \right) &= \varrho \left[-\frac{\varrho u_r}{4 - 3\gamma} \right. \\ &\left. + (2 - \gamma)(\gamma - 1) \xi + (\gamma - 1) u_r + \frac{2u_r^2}{\xi} \right] \end{aligned} \quad (18)$$

and

$$\begin{aligned} (\varrho^{\gamma-1} - u_r^2) \left(\frac{du_r}{d\xi} \right) &= \frac{\varrho u_r^2}{4 - 3\gamma} \\ - (2 - \gamma)(\gamma - 1) \xi u_r - (3 - 2\gamma) u_r^2 \\ &+ (4 - 3\gamma) \varrho^{\gamma-1} - \frac{2u_r}{\xi} \varrho^{\gamma-1}. \end{aligned} \quad (19)$$

Equations (18) and (19) are singular at the sonic point, $u_r^2 = \varrho^{\gamma-1}$. We obtain the the similarity solution by integrating equations (18) and (19) with the Runge-Kutta method. In the numerical integration we used the auxiliary variable of Whitworth, Summers (1985), s , defined by

$$\frac{\partial \xi}{\partial s} = \varrho^{\gamma-1} - u_r^2. \quad (20)$$

Using equation (20), we rewrite equations (18) and (19) into

$$\begin{aligned} \frac{d\varrho}{ds} &= \varrho \left[-\frac{\varrho u_r}{4 - 3\gamma} + (2 - \gamma)(\gamma - 1) \xi \right. \\ &\left. + (\gamma - 1) u_r + \frac{2u_r^2}{\xi} \right], \end{aligned} \quad (21)$$

and

$$\begin{aligned} \frac{du_r}{ds} &= \frac{\varrho u_r^2}{4 - 3\gamma} - (2 - \gamma)(\gamma - 1) \xi u_r \\ &- (3 - 2\gamma) u_r^2 + (4 - 3\gamma) \varrho^{\gamma-1} \\ &- \frac{2u_r}{\xi} \varrho^{\gamma-1}, \end{aligned} \quad (22)$$

respectively.

Similarity solutions exist for $\gamma < 4/3$. Figure 1 shows the similarity solutions for $\gamma = 0.9, 1.0$, and 1.1 . The solid curves denote ϱ while the dashed curves denote the infall velocity, $-u + (2 - \gamma)\xi$. These solutions are the same as those obtained by Yahil (1983) and Suto, Silk (1988).

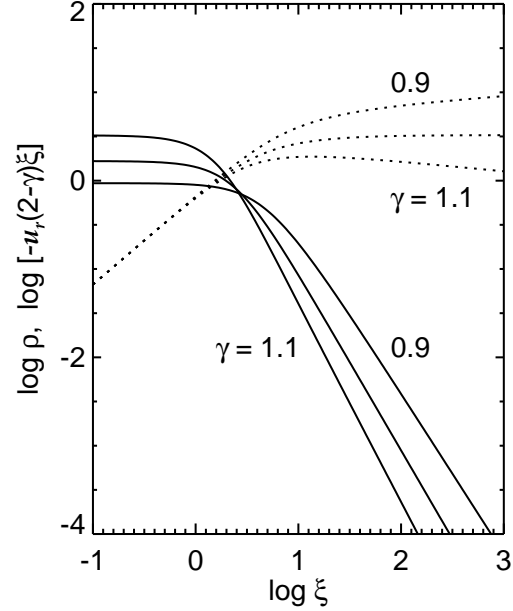


Fig. 1.. The similarity solutions are shown for $\gamma = 0.9, 1.0$, and 1.1 . The solid curves denote the density, ϱ . The dashed curves denote the infall velocity, $-u + (2 - \gamma)\xi$. The infall velocity does not include the apparent motion in the zooming coordinates and is positive for inward flow.

3. Bar Mode

In this section we consider a non-spherical perturbation around the similarity solution. The density perturbation is assumed to be proportional to the spherical harmonics, $Y_\ell^m(\theta, \varphi)$. Then the density and velocity are expressed as

$$\varrho = \varrho_0 + \delta\varrho(\xi) e^{\sigma\tau} Y_\ell^m(\theta, \varphi), \quad (23)$$

$$u_r = u_{r0} + \delta u_r(\xi) e^{\sigma\tau} Y_\ell^m(\theta, \varphi), \quad (24)$$

$$u_\theta = \delta u_\theta(\xi) \frac{e^{\sigma\tau}}{\ell + 1} \frac{\partial}{\partial \theta} Y_\ell^m(\theta, \varphi), \quad (25)$$

$$u_\varphi = \delta u_\theta(\xi) \frac{e^{\sigma\tau}}{(\ell + 1) \sin \theta} \frac{\partial}{\partial \varphi} Y_\ell^m(\theta, \varphi), \quad (26)$$

$$\phi = \phi_0 + \delta\phi(\xi) e^{\sigma\tau} Y_\ell^m(\theta, \varphi), \quad (27)$$

where the symbols with suffix, 0, denote the values in the similarity solution and the symbols with the symbol, δ , denote the perturbations. Substituting equations (24) throughout (27) into equations (12), (13), and (14), we obtain the perturbation equations,

$$\begin{aligned} (\sigma + 3\gamma - 4) \delta\varrho + \frac{1}{\xi^2} \frac{\partial}{\partial \xi} [\xi^2 (\varrho_0 \delta u_r + u_{r0} \delta\varrho)] \\ - \ell \frac{\varrho_0 \delta u_\theta}{r} = 0, \end{aligned} \quad (28)$$

$$(\sigma + 2\gamma - 3)\delta u_r + \frac{\partial}{\partial \xi}(u_{r0}\delta u_r) + \frac{\partial}{\partial \xi}\left(\frac{\delta \varrho}{\rho_0^{2-\gamma}}\right) + \delta \Gamma = 0, \quad (29)$$

$$(\sigma + 2\gamma - 3)\delta u_\theta + \frac{u_{r0}}{\xi}\frac{\partial}{\partial \xi}(\xi\delta u_\theta) + \frac{\ell + 1}{\xi}\left(\frac{\delta \varrho}{\rho_0^{2-\gamma}} + \delta \phi\right) = 0, \quad (30)$$

$$\frac{\partial}{\partial \xi}\delta \phi = \delta \Gamma, \quad (31)$$

and

$$\frac{\partial}{\partial \xi}\delta \Gamma = -\frac{2\delta \Gamma}{\xi} + \frac{\ell(\ell + 1)}{\xi^2}\delta \phi + \delta \varrho. \quad (32)$$

These perturbation equations have singularities at the origin ($\xi = 0$), the sonic point $[(u_{r0})^2 - \varrho^\gamma - 1]$, and the infinity ($\xi = +\infty$). These perturbation equations reduce to those of Hanawa, Matsumoto (1999) when $\gamma = 1$. We solve these perturbation equations as an eigenvalue problem for the growth rate, σ , according to them. The details of the numerical procedures are given in Hanawa, Matsumoto (1999). The growth rate is obtained as a function of γ and ℓ . The growth is independent of m since the unperturbed state is spherically symmetric (see, e.g., Hanawa, Matsumoto 1999).

Figure 2 shows the growth rate, σ , for $\ell = 2$ mode as a function of γ . The open squares denote the numerically obtained growth rates and the curve labeled ‘‘Bar’’ denotes a smooth fit to them. The growth rate is larger for smaller γ . A collapsing gas sphere is unstable only when $\gamma < 1.097$. We cannot find a damped mode since appropriate boundary condition are not given at $\xi = \infty$ for it (see appendix 2).

We searched for $\ell = 3$ mode but could find none. Although $\ell = 1$ mode exists, it denotes only the misfit to the center of gravity and is not relevant to real instability (Hanawa, Matsumoto 1999). A higher ℓ mode is also unlikely to exist. Thus only the bar mode gives a non-spherical density perturbation growing during the collapse. Since the bar mode is stabilized for $\gamma > 1.097$, a similarity solution for $\gamma > 1.097$ is stable against any non-spherical perturbation. This result can answer to the question posed by Goldreich, Lai, Sahriling (1997). They asked whether a dynamically collapsing iron resuting type II super nova is unstable against a large scale non-spherical perturbation. Since the dynamically collapsing iron core is well approximated by a similarity solution for $\gamma \simeq 4/3$, it is stable against any non-spherical density perturbation.

Figure 3 illustrates the variety of the bar mode. Each panel shows a dynamically collapsing isothermal gas cloud suffering a different bar mode perturbation. It

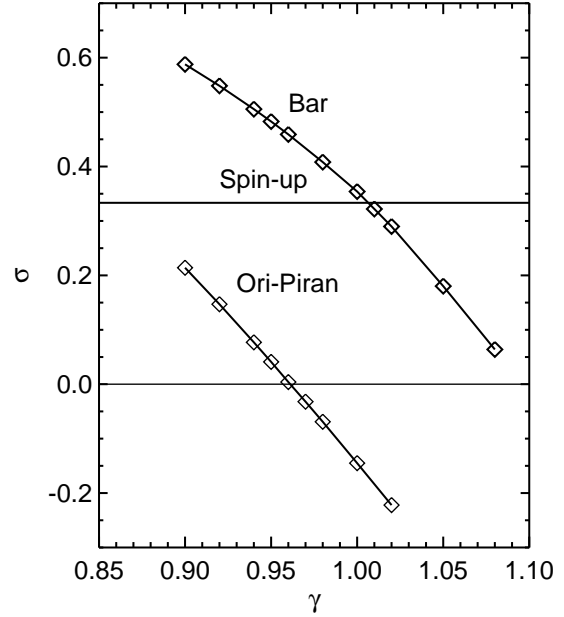


Fig. 2.. The growth rate, σ , is shown as a function of γ . The open squares denote numerically obtained data points.

shows the density distribution perspective by isodensity surfaces. Panel (a) denotes a bar mode of $m = 0$. In panel (a) the collapsing gas cloud is elongated in the z -direction. Panel (b) denotes the same bar mode of $m = 0$ but having the opposite sign. In panel (b) the collapsing gas cloud is oblate and compressed in the z -direction. Panels (c) and (d) denote the bar modes of $m = 1$ and 2 , respectively. When the modes grow, the collapsing gas cloud becomes triaxial.

4. Spin-up Mode

In this section we consider the velocity perturbation expressed as

$$\begin{pmatrix} u_r \\ u_\theta \\ u_\varphi \end{pmatrix} = \begin{bmatrix} \frac{A_{\ell, m}(\xi)}{\xi} \frac{\partial}{\partial \varphi} Y_\ell^m(\theta, \varphi) e^{\sigma \tau} \\ -\frac{A_{\ell, m}(\xi)}{\xi} \frac{\partial}{\partial \theta} Y_\ell^m(\theta, \varphi) e^{\sigma \tau} \end{bmatrix} \quad (33)$$

Substituting equation (33) into equation (12) we obtain

$$\delta \varrho = 0, \quad (34)$$

for this mode. Similarly we obtain

$$\delta \phi = 0, \quad (35)$$

by substituting equation (34) into equation (14). Substituting equations (33), (34), and (35) into equation (13),

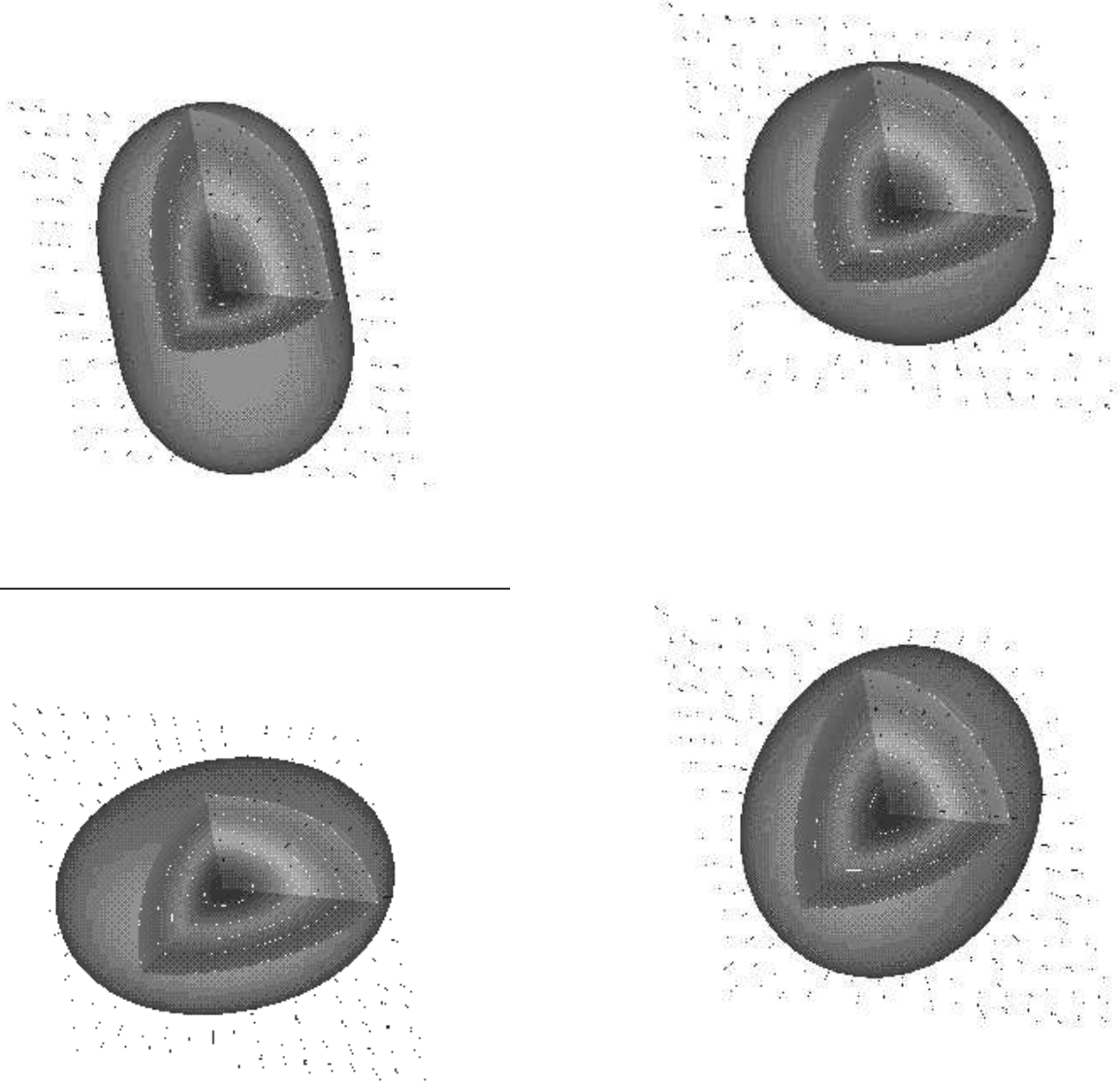


Fig. 3.. A collapsing isothermal cloud core suffering the bar mode. The density distribution is shown by the isodensity surfaces. The velocity in the $x - z$ plane is shown by arrows. Each panel shows a different bar mode. Panel (a) denotes the bar mode of $m = 0$. Panel (b) denotes the same bar mode of $m = 0$ but having the opposite sign. Panel (c) denotes the bar mode of $m = 1$ while panel (d) does that of $m = 2$. In panels (a) and (b) the perturbation is added so that the radial velocity is $v_r \propto [-2/3 \pm 0.10(3 \cos^2 \theta - 1)]r$ near the center, respectively. In panel (c) the radial velocity is $v_r \propto (-2/3 + 0.05 \sin 2\theta \cos \varphi)r$ near the center. In panel (d) it is $v_r \propto (-2/3 + 0.10 \sin^2 \theta \cos 2\varphi)r$ near the center.

we obtain

$$(\sigma - 7 + 5\gamma) \varrho_0 A_{\ell,m} + \frac{1}{\xi^2} \frac{\partial}{\partial \xi} (\xi^2 \varrho_0 u_{r0} A_{\ell,m}) = 0 . (36)$$

Substituting equation (15) into equation (36), we obtain

$$(\sigma - 3 + 2\gamma) A_{\ell,m} + u_{r0} \frac{\partial}{\partial \xi} (A_{\ell,m}) = 0 . (37)$$

Substituting equation (A2) into equation (37) we obtain

$$\begin{aligned} \sigma &= 3 - 2\gamma + \left(\gamma - \frac{4}{3} \right) \frac{d \ln A_{\ell,m}}{d \ln \xi} \Big|_{\xi=0} \\ &= \frac{1}{3} + \left(\gamma - \frac{4}{3} \right) \left(\frac{d \ln A_{\ell,m}}{d \ln \xi} \Big|_{\xi=0} - 2 \right) . (38) \end{aligned}$$

The growth rate, σ , should be smaller than $1/3$ since the velocity perturbation is regular at the origin only for $d \ln A_{\ell,m}/d \ln \xi \geq 2$ [see equation (33)]. When $d \ln A_{\ell,m}/d \ln \xi = 2$, the angular velocity is nearly constant around the origin. The growth rate of the spin-up mode, $\sigma = 1/3$ is also shown in Figure 2 for comparison with that of the bar mode. This spin-up mode is essentially the same as the spin-up mode shown in Appendix of Hanawa, Nakayama (1997).

5. Ori-Piran Mode

In this section we consider a perturbation emanating from the sonic point. According to Ori, Piran (1988) we analyze a spherical perturbation which vanishes inside the sonic point. Substituting $\ell = 0$ into equations (24) through (27) we obtain

$$\frac{\partial}{\partial \tau} \delta \varrho + \frac{1}{\xi^2} \frac{\partial}{\partial \xi} [\xi^2 (\delta \varrho u_{r0} + \varrho_0 \delta u_r)] = (4 - 3\gamma) \delta \varrho, \quad (39)$$

$$\begin{aligned} \frac{\partial}{\partial \tau} \delta u_r + \frac{\partial u_{r0}}{\partial \xi} \delta u_r + u_{r0} \frac{\partial}{\partial \xi} \delta u_r \\ - (\varrho_0)^{\gamma-3} \frac{\partial \varrho_0}{\partial \xi} \delta \varrho + \frac{1}{\varrho_0} \frac{\partial}{\partial \xi} [(\varrho_0)^{\gamma-1} \delta \varrho] \\ + \delta \Gamma = (3 - 2\gamma) \delta u_r, \end{aligned} \quad (40)$$

and

$$\delta \Gamma = \frac{1}{\xi^2} \int_0^\xi \delta \varrho(\zeta) \zeta^2 d\zeta. \quad (41)$$

We evaluate equations (39), (40), and (41) at the sonic point. Then we obtain

$$\varrho_0 \frac{\partial}{\partial \xi} \delta u_r + u_{r0} \frac{\partial}{\partial \xi} \delta \varrho = 0, \quad (42)$$

$$u_{r0} \frac{\partial}{\partial \xi} \delta u_r + (\varrho_0)^{\gamma-2} \frac{\partial}{\partial \xi} \delta \varrho = 0, \quad (43)$$

$$\delta \phi = 0, \quad (44)$$

at the sonic point. Equations (42) and (43) are equivalent and indicate that the sound wave traveling outwards with the phase speed $u_r + c_s$ vanishes. In other words the perturbation emanating from the sonic point is the other sound wave of which phase velocity is zero at the sonic point, $u_r - c_s = 0$. Taking the linear combination of the ξ -derivatives of equations (39) and (40) and evaluating it at the sonic point, we obtain

$$\begin{aligned} \frac{\partial}{\partial \tau} \left(u_{r0} \frac{\partial}{\partial \xi} \delta \varrho - \varrho_0 \frac{\partial}{\partial \xi} \delta u_r \right) - \left[-2 \frac{\partial u_{r0}}{\partial \xi} \right. \\ \left. + (\gamma - 1) u_{r0} \frac{\partial \ln \varrho_0}{\partial \xi} + \left(\frac{7 - 5\gamma}{2} \right) \right] \\ \times \left(u_{r0} \frac{\partial}{\partial \xi} \delta \varrho - \varrho_0 \frac{\partial}{\partial \xi} \delta u_r \right) = 0 \end{aligned} \quad (45)$$

where equations (42) and (43) are substituted. Equation (45) means

$$\sigma = -2 \frac{\partial u_{r0}}{\partial \xi} + (\gamma - 1) u_{r0} \frac{\partial \ln \varrho_0}{\partial \xi} + \left(\frac{7 - 5\gamma}{2} \right). \quad (46)$$

When $\gamma = 1$, equation (46) is equivalent to equation (15). To elucidate the growth (or damping) of this mode we rewrite equation (46) into

$$\sigma = -2 \frac{\partial}{\partial \xi} (u_{r0} - c_s) + \left(\frac{7 - 5\gamma}{2} \right). \quad (47)$$

The first term in the right hand side of equation (47) denotes the dilution of the wave due to the spatial variation of the phase velocity. The phase speed vanishes at the sonic point and increases with the radial distance. Thus the wave dilutes and the amplitude decreases. The second term in equation (47) denotes the self-reproduction. As shown in the right hand side of equations (12) and (13), the density and momentum density reproduce and amplify themselves when measured in the zooming coordinates. When the self-reproduction overcomes the dilution, the collapsing gas sphere is unstable against the Ori-Piran mode.

Nonlinear growth of the Ori-Piran mode has not been studied yet. This is the first report that a similarity solution of collapsing gas sphere can be unstable against the Ori-Piran mode. As far as we know, Ogino, Tomisaka, Nakamura (1999) is the first report on collapse of a polytropic gas sphere with $\gamma < 1$. They reported a little on their numerical simulations of $\gamma < 1$ and mentioned nothing on the Ori-Piran instability. Since the similarity solution is unstable, their numerical solution may not be well approximated by it.

6. Summary

As shown in the previous sections a gravitationally collapsing polytropic gas sphere can suffer from three types of instability. When $\gamma < 4/3$, it is unstable against spin-up mode shown in section 5. The spin-up mode grows in proportion to $|t - t_0|^{-1/3}$ and accordingly in proportion to $\rho^{1/6}$. When $\gamma < 1.097$, it is unstable also against the bar mode instability. The growth rate of the bar mode is large for smaller γ . When $\gamma < 1.006$, it is larger than that of the spin-up mode. When $\gamma \leq 0.961$, a gravitationally collapsing polytropic gas sphere is unstable also against the Ori-Piran mode.

It is particularly interesting that the bar mode has a larger growth rate when γ is smaller. This means that the bar mode grows faster when the sound speed decreases with the increase in the density. This result may be valid also for a gravitationally collapsing gas sphere in which turbulence has an effective pressure. Since the effective sound speed is lower in a denser part of molecular cloud,

a collapsing cloud core may be more unstable against the bar mode than a purely isothermal gas sphere. This enhancement in the bar mode instability may be relevant to fragmentation of a collapsing cloud core and formation of multiple stars during the collapse.

We thank Naoya Fukuda and Kazuya Saigo for useful discussion and their help for making figures. This research is financially supported in part by the Grant-in-Aid for Scientific Research (C) of the Ministry of Education, Science, Sports and Culture (No. 09640318) and by the Grant-in-Aid for Scientific Research on Priority Areas of the Ministry of Education, Science, Sports and Culture of Japan (No. 10147105).

Appendix 1. Similarity Solution for Collapse of Polytopic Gas Sphere

In this appendix we summarize the main characteristics of the similarity solution for collapse of polytopic gas sphere. See Yahil (1983) and Suto, Silk (1988) for the derivation and more details.

When we expand the similarity solution around $\xi = 0$ by the Taylor series, they are expressed as

$$\varrho(\xi) = \varrho_0(0) - \frac{[\varrho_0(0)]^{2-\gamma}}{6\gamma} \left[\varrho_0(0) - \frac{2}{3} \right] \xi^2 + \mathcal{O}(\xi^2), \quad (\text{A1})$$

and

$$u_r(\xi) = \left[(2-\gamma) - \frac{2}{3} \right] \xi + \frac{[\varrho_0(0)]^{1-\gamma}}{15\gamma} \times \left(\varrho_0 - \frac{2}{3} \right) \left(\frac{4}{3} - \gamma \right) \xi^3 + \mathcal{O}(\xi^5). \quad (\text{A2})$$

In the region of $\xi \gg 1$ the similarity solution has the asymptotic form of

$$\varrho \propto \xi^{-2/(2-\gamma)}, \quad (\text{A3})$$

and

$$[u_r - (2-\gamma)\xi] \propto \xi^{(1-\gamma)/(2-\gamma)}. \quad (\text{A4})$$

Appendix 2. Asymptotic Behavior of Bar Mode Perturbation

We can derive the asymptotic forms for the bar mode perturbation from the requirement that the perturbation is regular at $\xi = 0$. The density and velocity perturbations around $\xi = 0$ are expressed as

$$\delta\varrho = \alpha [\varrho_0(0)]^{2-\gamma} \xi^\ell \quad (\text{A5})$$

$$\delta u_r = \beta \ell \xi^{\ell-1} \quad (\text{A6})$$

$$\delta u_\theta = \beta (\ell + 1) \xi^{\ell-1} \quad (\text{A7})$$

$$\delta\phi = -\{\alpha + [\sigma + 2\gamma - 3$$

$$+ \frac{\ell(4-3\gamma)}{3}] \beta\} \xi^\ell, \quad (\text{A8})$$

where α and β are free parameters. When we derive the above Taylor series expansion, we use equation (A2). The derivation is essentially the same as that shown in Hanawa, Matsumoto (1999).

As a boundary condition we assume that the relative density perturbation, $\delta\varrho/\varrho_0$, is vanishingly small at infinity, $\xi = \infty$. After some algebra we obtain the asymptotic relations,

$$\frac{\delta\varrho}{\varrho_0} \propto \xi^{-\sigma/(2-\gamma)} \quad (\text{A9})$$

$$\delta u_r \propto \xi^{-(\sigma+\gamma-1)/(2-\gamma)}, \quad (\text{A10})$$

$$\delta u_\theta \propto \xi^{-(\sigma+\gamma-1)/(2-\gamma)}, \quad (\text{A11})$$

$$\phi \propto \xi^{-(\sigma-2\gamma+2)/(2-\gamma)}, \quad (\text{A12})$$

and

$$\phi = \left[\frac{(\sigma-2\gamma+2)(\sigma-3\gamma+4)}{(2-\gamma)^2} - \ell(\ell+1) \right]^{-1} r^2 \delta\varrho. \quad (\text{A13})$$

When we derive the above relations, we use equations (A3) and (A4). See also Hanawa, Matsumoto (1999) for the derivation.

References

- Bouquet S., Feix M. R., Fijalkow E., Munier A. 1985, ApJ 293, 494
 Goldreich P., Lai D., Sahrling, M. 1997, in *Unsolved Problems in Astrophysics*, ed. J. Bahcall, J. P. Ostriker (Princeton Univ. Press, Princeton) p269
 Hanawa, T., Matsumoto, T., 1999, ApJ 521, in press
 Mathieu, R. D. 1994, ARA& 32, 465
 Matsumoto, T., Hanawa, T. 1999, ApJ 521, in press
 Ori A., Piran T. 1988, MNRAS, 234, 821
 Ostriker J. 1964, ApJ 140, 1056
 Silk J., Suto Y. 1988, ApJ, 335, 295
 Suto Y., Silk J. 1988, ApJ 326, 527
 Truelove, J. K., Klein, R. I., McKee, C. F., Holliman, J. H., II, Howell, L. H., Greenough, J. A. 1997, ApJ 489, L179
 Truelove, J. K., Klein, R. I., McKee, C. F., Hollman, J. H., II, Howell, L. H., Greenough, J. A., Woods, D. T. 1998, ApJ 495, 821
 Whitworth A., Summers D. 1985, MNRAS 214, 1
 Yahil A. 1983, ApJ 265, 1047